Check for updates

Journal of Geophysical Research: Oceans

RESEARCH ARTICLE
10.1029/2018JC014549

Key Points:
- We present a decade-long seasonal hydrographic time series from a major Greenland tidewater outlet glacial fjord
- The fjord's seasonal circulation system damps the coastal temperature signal in the fjord
- Mean temperature shifts in the inner fjord are predominantly linked to local coastal water masses and can be related to local atmospheric forcing

Correspondence to:
J. Mortensen,
jomo@natur.gl

Citation:
Mortensen, J., Rysgaard, S., Arendt, K. E., Juul-Pedersen, T., Søgaard, D. H., Bendtsen, J., & Meire, L. (2018). Local coastal water masses control heat levels in a West Greenland tidewater outlet glacier fjord. *Journal of Geophysical Research: Oceans, 123*, 8068–8083. https://doi.org/10.1029/2018JC014549

Received 6 SEP 2018
Accepted 8 OCT 2018
Accepted article online 15 OCT 2018
Published online 9 NOV 2018

©2018. The Authors.
This is an open access article under the terms of the Creative Commons Attribution-NonCommercial-NoDerivs License, which permits use and distribution in any medium, provided the original work is properly cited, the use is non-commercial and no modifications or adaptations are made.

Local Coastal Water Masses Control Heat Levels in a West Greenland Tidewater Outlet Glacier Fjord

J. Mortensen[1], S. Rysgaard[1,2,3], K. E. Arendt[1,4], T. Juul-Pedersen[1], D. H. Søgaard[1,3], J. Bendtsen[5], and L. Meire[1,6]

[1]Greenland Climate Research Centre, Greenland Institute of Natural Resources, Nuuk, Greenland, [2]Centre for Earth Observation Science, CHR Faculty of Environment Earth and Resources, University of Manitoba, Winnipeg, Manitoba, Canada, [3]Arctic Research Centre, Aarhus University, Aarhus, Denmark, [4]SCIENCE, Private and Public Sector Services, University of Copenhagen, Frederiksberg, Denmark, [5]ClimateLab, Copenhagen, Denmark, [6]Department of Estuarine and Delta Systems, NIOZ Royal Netherlands Institute of Sea Research and Utrecht University, Yerseke, Netherlands

Abstract Fjords form the gateway between the open ocean and the Greenland Ice Sheet (GIS) and consequently play a crucial role for the stability of the Ice Sheet. Hydrographic observations, especially with seasonal resolution, from these fjords are limited making it difficult to assess linkages between the fjord, coastal water masses, and freshwater discharge from GIS. Here we present a decade-long monthly hydrographic time series from a southwest Greenland fjord in direct contact with GIS. Our observations reveal significant temporal and spatial water mass variations related to coastal, glacial, and atmospheric dynamics. During winter, the fjord circulation is dominated by seasonal dense coastal inflows and the timing of these inflows determines intermediate and deepwater temperatures. During summer, runoff from GIS leads to a pronounced freshening of the fjord. In general, the fjord's seasonal circulation system damps the seasonal variation in temperature in the fjord. This leads to a seasonal temperature range in the intermediate layer in the inner part of the fjord that is half the observed range at the fjord entrance. Changes in mean water temperatures in the intermediate layer seem predominantly linked to local coastal water masses, where cold winter/warm summer events decrease/increase the mean water temperatures. Consequently, these events play an important role in heat transport toward glacier termini.

Plain Language Summary Fjords form the gateway between warm open ocean water and the Greenland Ice Sheet and play a crucial role for the stability of the Ice Sheet. Temperature and salinity observations from these fjords are limited, making it difficult to understand the link between the fjord, coastal water masses, and freshwater discharge from the Ice Sheet. We present a decade-long monthly temperature and salinity time series from a southwest Greenland fjord in direct contact the Ice Sheet. Our data reveal that changes in mean water temperatures in the water mass responsible for melting the Ice Sheet is linked to local coastal water masses, where cold winter events decrease and warm summer events increase the mean water temperatures close to marine terminating glaciers.

1. Introduction

The accelerated retreat of many tidewater outlet glaciers in Greenland has motivated recent fjord studies to assess the heat transport from relatively warm open ocean or coastal water masses to the tidewater outlet glaciers in the inner parts of fjords (Bendtsen et al., 2015; Mortensen et al., 2011; Motyka et al., 2011; Straneo et al., 2010; Sutherland & Straneo, 2012). Even though relatively warm open ocean water has been observed at entrances to tidewater outlet glacier fjords, little is known about water masses at fjord entrances and in the proximity of tidewater outlet glaciers, renewal rates, and their temporal connections with coastal water masses (e.g., Gladish et al., 2015; Jackson et al., 2014; Mortensen et al., 2013). One of the key questions is how hydrographic changes observed at the entrance of a fjord are transmitted through the fjord system to the glacier terminus (Mortensen et al., 2014). Models of conceptual fjord systems show a strong impact of warm coastal water on glacier dynamics (e.g., Carroll et al., 2017). However, validation of these conceptually modeled fjord systems is often lacking as seasonal observations from fjords in Greenland are sparse, and only a few fjord systems have been studied extensively year-round, for example, Young Sound (Boone et al., 2018; Rysgaard & Glud, 2007), Godthåbsfjord (Mortensen et al., 2011, 2013), Sermilik, and Kangerlussuaq Fjords (Jackson et al., 2014).

21699291, 2018, 11, Downloaded from https://agupubs.onlinelibrary.wiley.com/doi/10.1029/2018JC014549 by EVIDENCE AID - BELGIUM, Wiley Online Library on [20/02/2023]. See the Terms and Conditions (https://onlinelibrary.wiley.com/terms-and-conditions) on Wiley Online Library for rules of use; OA articles are governed by the applicable Creative Commons License

21699291, 2018, 11, Downloaded from https://agupubs.onlinelibrary.wiley.com/doi/10.1029/2018JC014549 by EVIDENCE AID - BELGIUM, Wiley Online Library on [20/02/2023]. See the Terms and Conditions (https://onlinelibrary.wiley.com/terms-and-conditions) on Wiley Online Library for rules of use; OA articles are governed by the applicable Creative Commons License

The exchange of water masses between fjords, coastal areas, and the open ocean has a major impact on the environmental conditions in Greenland fjords. Temperature and salinity gradients along the fjords are regulated by the fjords' seasonal circulation systems and their various physical drivers (Mortensen et al., 2011, 2014). Besides being important components for melting of the Greenland Ice Sheet (GIS) and associated global sea level rise, these seasonal circulation systems determine biological parameters: changes in fjord circulation and physical drivers seem to explain spatial gradients in metazooplankton communities (Arendt et al., 2013; Tang et al., 2011) and seasonal variations in phytoplankton species composition and primary production (Juul-Pedersen et al., 2015; Krawczyk et al., 2015; Meire et al., 2016). Biogeochemical gradients generated by these circulation systems also influence the exchange of properties between fjords and the open ocean: Rysgaard et al. (2012) found that the mixing of surface water inside the fjord with coastal water masses regulated the air-sea gas exchange of CO_2 in Godthåbsfjord during summer. The presence of marine-terminating glaciers was found to explain sustained high productivity in fjords in Greenland (Meire et al., 2017). Interpretation of paleo-climatic proxies from fjords in Greenland (e.g., Versteegh et al., 2012) similarly depends on a knowledge of spatial gradients toward the open ocean. Thus, the exchange between the fjord and the open ocean and the link between this exchange and the fjord's seasonal circulation system is important for understanding physical conditions, biogeochemical cycling, and ecosystem dynamics inside fjords around Greenland.

In this paper, we present along-fjord observations based on seasonal hydrographic time series from the outer parts of Godthåbsfjord (close to the fjord entrance) and the inner parts (in the vicinity of tidewater outlet glaciers). These time series are relevant for studying the interaction between the open ocean and the inner fjord because of the presence of three tidewater outlet glaciers in direct connection with GIS. We first describe the hydrographic setting of the fjord in relation to the location of the time series and present a water mass analysis for the outer and inner parts of the fjord. We then present the average conditions of temperature and salinity at the fjord entrance in relation to seasonal changes in local air temperatures and freshwater (FW) runoff. Finally, we analyze the seasonal pattern and interannual variability of water masses observed at the entrance to and inside the fjord and relate these to variations in local coastal water masses and atmospheric forcing.

2. Study Area and Methodology

Godthåbsfjord (Nuup Kangerlua) is located in Southwest Greenland and is among the largest fjord systems in Greenland in terms of surface area. The main fjord branch is 190 km long, and the fjord system covers an area of 2,013 km^2 (Figure 1). Godthåbsfjord is in contact with three marine-terminating glaciers and three land-terminating glaciers from GIS. The grounding line depths of the three tidewater outlet glaciers have been estimated to $<$250, $<$140, and $<$160 m for Kangiata Nunaata Sermia, Akullersuup Sermia, and Narsap Sermia, respectively. Due to an adjacent sill in front of Kangiata Nunaata Sermia and Akullersuup Sermia, we define the *glacial melt domain* for a fjord, as the depth range, water masses must enter to reach the tidewater outlet glacier and potentially be available for melt. The glacial melt domain is determined by the layer between the sea surface and the glacier grounding line, or the adjacent sill depth in case it is shallower than the glacier grounding line (Mortensen et al., 2014). Sill 3 has a depth of ~160 m, and in Godthåbsfjord the glacial melt domain then is defined from 0- to 160-m depth (Figure 2).

The present study is based on three hydrographic time series located in three different physical and dynamic domains: the inner fjord, the outer fjord, and in coastal waters. The location of the innermost sampling station contributing to the inner fjord time series is usually determined by the sea ice edge or the density of the glacial ice field cover during monthly cruises in the fjord. The stations between GF7 and GF17 represent the inner fjord region, with the majority of stations being located in the region between GF12 and GF14 (indicated by the closed blue area in Figure 1). Some of the winter observations were obtained during work on the sea ice and in the ice mélange in the innermost part of the fjord.

The outer fjord time series is based on measurements from the GF3 monitoring station located in the outer sill region of the fjord (64°07′N, 51°53′W, bottom depth: ~360 m; Figure 1). This region is characterized by a sequence of relatively deep sills near Nuuk. The entrance (main) sill to the fjord system has a depth of ~200 m (198 ± 4 m; recent bathymetric measurements show that the main sill is 30 m deeper than earlier reported by Mortensen et al., 2011), and the next sill toward the fjord, referred to as Sill 1, has a depth of 250 m (Figure 2). The width of the fjord at Sill 1 is ~5 km. The tidal range varies between 1 and 5 m (Richter et al., 2011), and a total volume of ~20 km^3 of water passes a cross section at Nuuk during a single tidal cycle at spring tide. This

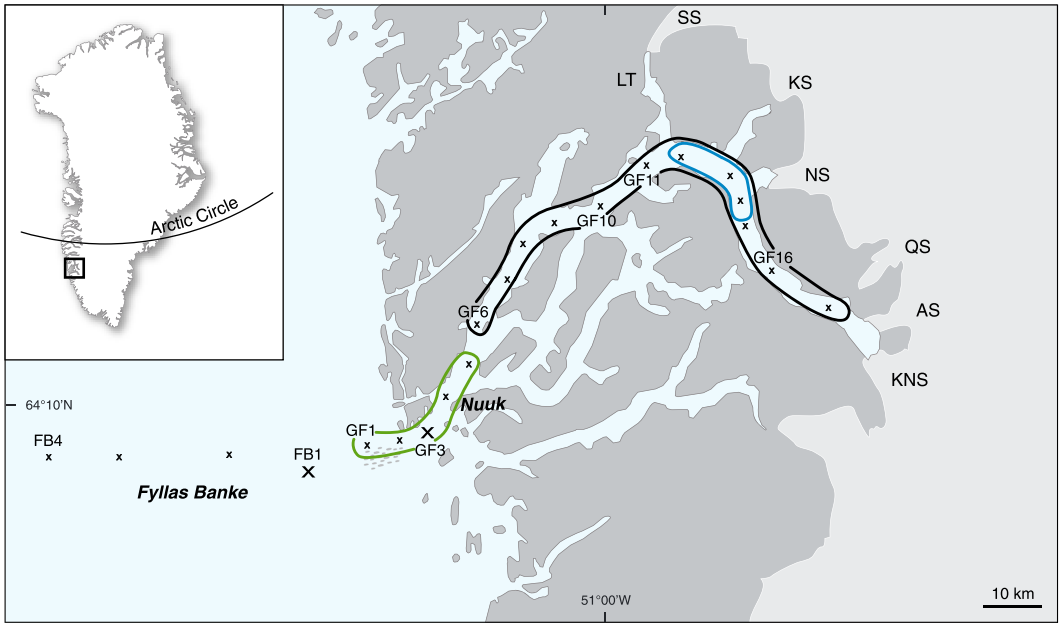

Figure 1. Map of the Godthåbsfjord system and the adjacent continental shelf and slope, showing standard hydrographic stations as crosses. The coastal station (FB1) and outer fjord station (GF3) are shown as larger crosses. The outer sill region, main fjord branch, and approximate mean position of the inner fjord station are indicated as green, black, and blue closed areas, respectively. KNS, Kangiata Nunaata Sermia; AS, Akullersuup Sermia; NS, Narsap Sermia; QS, Qamanaarsuup Sermia; KS, Kangilinnguata Sermia; SS, Saqqap Sermersua; LT, Lake Tasersuaq.

amount of water is comparable to the total annual liquid freshwater runoff into the fjord (Langen et al., 2015; Motyka et al., 2017). The outer sill region is characterized by intense diapycnal mixing and strong tidal currents with surface drift velocities close to 1 m/s at spring tides (observed during station occupations). A more moderate tidal velocity field is observed inside the fjord, with the dominant semidiurnal M_2 constituent having an amplitude of around 5 cm/s (Mortensen et al., 2014). GF3 has been sampled monthly since October 2005.

The coastal time series is made up by the Fyllas Banke standard hydrographic monitoring station FB1 (63°57′N, 52°22′W, bottom depth: ~273 m), visited 2–3 times each year in the period of 2005–2016. The coastal station FB1 is located in a trough on the continental shelf. This trough is part of the canyon system surrounding Fyllas Banke, which connects the continental slope with the fjord entrance.

The seasonal circulation system is characterized by four circulation modes with different driving forces. Figure 2 summarizes our present knowledge of the seasonal circulation system and distribution of water masses in Godthåbsfjord. Two of the circulation modes are associated with freshwater discharge during the summer melt season (i.e., runoff and subglacial freshwater (SgFW) discharge indicated by blue arrows in Figure 2a): the shallow estuarine circulation driven by runoff and the deeper reaching subglacial circulation driven by subglacial freshwater discharge. One mode is referred to as the intermediate baroclinic circulation (red arrows in Figures 2a and 2b) driven by tidal-induced diapycnal mixing in the outer sill region near GF3. This mixing causes a horizontal density gradient between the outer sill region and the main fjord and drives the intermediate baroclinic circulation. This circulation mode is present year-round. The last circulation mode is referred to as dense coastal inflows (blue arrows in Figure 2b) driven by density differences between coastal water masses and water masses in the fjord. This circulation mode renews basin water masses in the main fjord branch. The fjord-coast exchange above the fjords entrance (main) sill is not shown as very few data exist from this area.

Two heat sources for glacial melt have been identified for Godthåbsfjord: a regional and a local. Below we distinguish between regional and local water masses as water masses formed outside or inside the southwest Greenland continental shelf, respectively (we consider the fjords as part of the continental shelf). The regional heat source is associated with dense coastal inflow of modified subpolar mode water (SPMW) and the formation of a new basin water type (BW_4) replacing an older basin water type (BW_2) indicated in Figure 2b (e.g.,

21699291, 2018, 11, Downloaded from https://agupubs.onlinelibrary.wiley.com/doi/10.1029/2018JC014549 by EVIDENCE AID - BELGIUM, Wiley Online Library on [20/02/2023]. See the Terms and Conditions (https://onlinelibrary.wiley.com/terms-and-conditions) on Wiley Online Library for rules of use; OA articles are governed by the applicable Creative Commons License

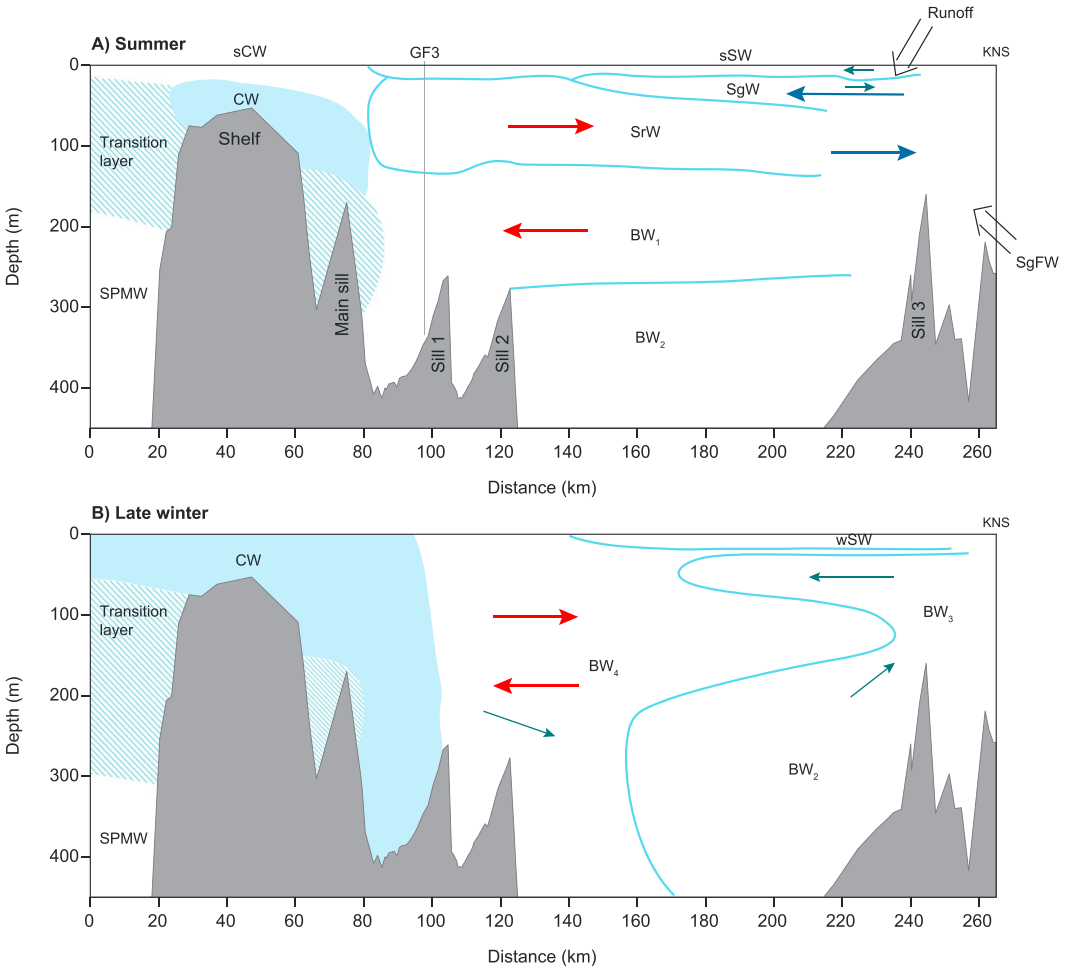

Figure 2. Schematic representation of present knowledge of the seasonal circulation system and distribution of water masses in Godthåbsfjord during (a) summer and (b) late winter (based on Mortensen et al., 2011, 2013, 2014). CW, coastal water; sCW, summer coastal water; SPMW, subpolar mode water; BW_i, basin water types i = 1–4 (see text for explanation); SrW, sill region water; SgW, subglacial water; sSW, summer surface water; wSW, winter surface water; SgFW, subglacial freshwater; KNS, Kangiata Nuaata Sermia. Estuarine circulation driven by runoff, small blue arrows in (a); subglacial circulation driven by SgFW discharge, large blue arrows in (a); intermediate baroclinic circulation, red arrows in (a) and (b); dense coastal inflows, blue arrows in (b). For more information on the two latter circulation modes see text. Location of the hydrographic monitoring station GF3 is shown in (a).

Holland et al., 2008). The local heat source is associated with the formation of sill region water (SrW) indicated in Figure 2a. A second local heat source is warm and less dense coastal water that enters the fjord's intermediate layer in autumn (the intermediate layer is located between the shallow surface layer and the basin layer below sill depth). A remnant of the local heat source is seen in Figure 2b as the basin water type (BW_3).

Conductivity, temperature, and depth measurements were collected using Sea-Bird Electronics SBE19plus SEACAT Profilers. The sensors were calibrated by the manufacturer on an annual basis, and precision of salinity was typically within 0.005–0.010. All profiles were averaged vertically in 1-m intervals.

3. Results and Discussion

3.1. Hydrographic Setting of the Main Fjord Branch

Figure 3 shows the hydrographic setting of the main fjord branch and the adjacent continental shelf and slope in the first part of May 2013. The outer fjord time series (GF3) is located in a region with weak vertical and horizontal property gradients, with a potential temperature and salinity of ~1 °C and ~33.4, respectively. The region between the main sill and Sill 2 is referred to as the outer sill region. Tidal mixing is responsible for

21699291, 2018, 11, Downloaded from https://agupubs.onlinelibrary.wiley.com/doi/10.1029/2018JC014549 by EVIDENCE AID - BELGIUM, Wiley Online Library on [20/02/2023]. See the Terms and Conditions (https://onlinelibrary.wiley.com/terms-and-conditions) on Wiley Online Library for rules of use; OA articles are governed by the applicable Creative Commons License

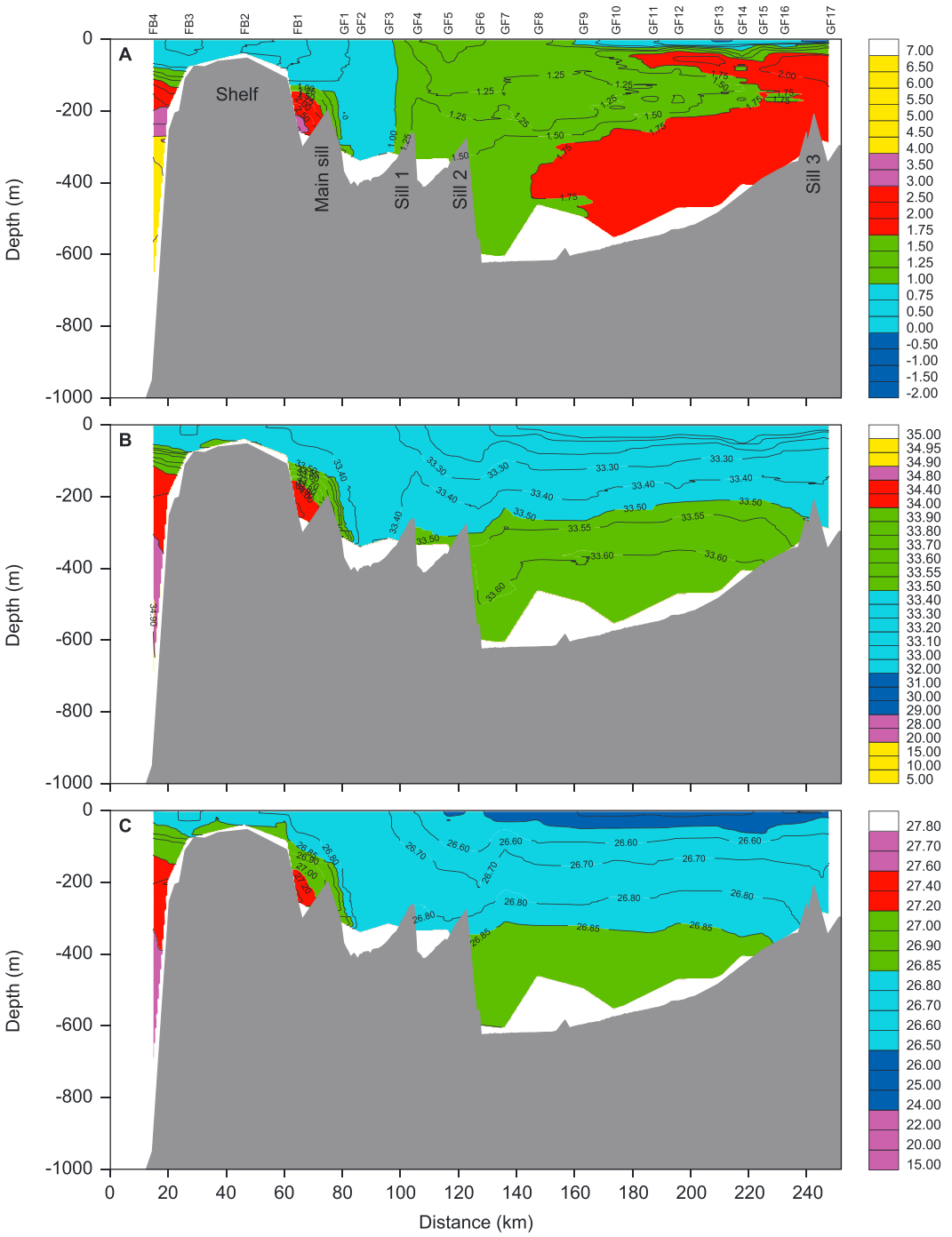

Figure 3. (a) Potential temperature (°C), (b) salinity, and (c) potential density anomaly (kg/m^3) of a length section from the continental slope (left), following the main fjord branch of Godthåbsfjord to the inner part near KNS in first part of May 2013.

the homogeneous conditions in this part of the fjord. A dense coastal inflow across the entrance (main) sill in the layer close to the bottom was observed during the occupation of the section. However, this inflow was only detectable at the first fjord station, GF1.

The inner time series (represented by GF17 on 8 May 2013; Figure 3) is located in a region from Sill 2 to the innermost part of the fjord, referred to as the main fjord branch. This part of the fjord was characterized by salinity (and thereby density), which increased gradually with depth from below the winter halocline,

21699291, 2018, 11, Downloaded from https://agupubs.onlinelibrary.wiley.com/doi/10.1029/2018JC014549 by EVIDENCE AID - BELGIUM, Wiley Online Library on [20/02/2023]. See the Terms and Conditions (https://onlinelibrary.wiley.com/terms-and-conditions) on Wiley Online Library for rules of use; OA articles are governed by the applicable Creative Commons License

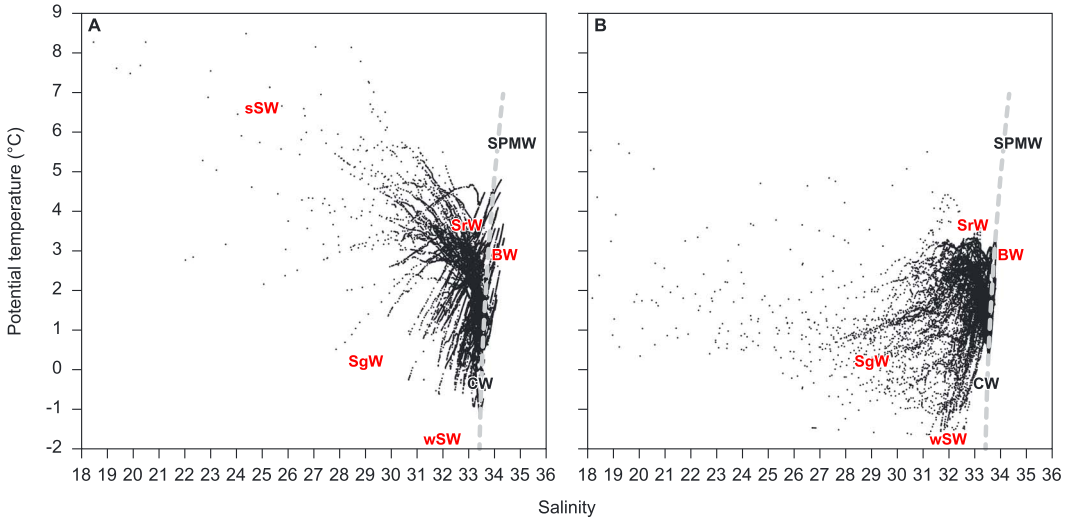

Figure 4. θ-S plot for (a) outer and (b) inner time series in the period of October 2005 to July 2016. Only data points in the 1- to 300-m depth range are shown for the inner time series in (b). The broken light grey line is the 26.9 isopycnal. Two of the three principal water masses (subpolar mode water [SPMW] and coastal water [CW]) are shown in black, and fjord water masses (summer surface water [sSW], winter surface water [wSW], subglacial water [SgW], sill region water [SrW], and basin water [BW]) are shown in red. The position of the final principal water mass freshwater (FW) in (a) and (b) is not shown but is located near (θ, S) = (0, 0). Measurements with salinity less than 18 are not shown in (b).

located at ~20-m depth (salinity increasing from 33.0 to 33.7), and with weak horizontal gradients. The temperature distribution was observed to be more complex, with relatively large horizontal and vertical gradients. The innermost parts of the fjord were characterized by temperatures above 2 °C in the intermediate water masses. Surface layer temperatures were ~0 °C.

The coastal time series (FB1) is located outside the fjord's entrance (main) sill in a region with weak vertical stratification in both temperature and salinity in the surface layer. Significant vertical gradients in both temperature and salinity were observed in the winter pycnocline, located between 50- to 300-m depth. Temperatures above the winter pycnocline were ~0.5 °C, whereas higher temperatures of 4–5 °C were observed below the winter pycnocline with a temperature maximum at 400-m depth (Figure 3a). Salinity above the winter pycnocline were ~33.5 compared with ~34.9 below the winter pycnocline.

3.2. Coastal and Fjord Water Masses

Figure 4 shows all conductivity, temperature, and depth records collected at the entrance to the fjord system (GF3), and the inner fjord time series in potential temperature-salinity (θ-S) diagrams. Three principal water masses dominate the fjord: subpolar mode water, coastal water (CW), and freshwater. Subpolar mode water and coastal water have their origins outside the fjord, whereas freshwater is associated with runoff, subglacial freshwater discharge, and precipitation. Five previously defined Godthåbsfjord water masses are shown in red: summer surface water (sSW), winter surface water (wSW), subglacial water (SgW), sill region water, and basin water. These water masses are the mixing product of the three principal water masses, modified by atmospheric heat exchange, freezing, and melting processes.

The warm and saline subpolar mode water is North Atlantic winter mode water that enters the fjord in a diluted form (Figure 4a). As it reaches the inner parts of the fjord, it loses its distinct characteristics and becomes part of the fjord's basin water. Coastal water is cold and less saline and considered formed during winter over the West Greenland continental shelf. It is observed to reach the outer fjord at GF3 in almost-undiluted form during winter.

During summer, when subglacial freshwater discharge is large, subglacial water is formed next to marine-terminating glaciers and found below the fresh summer surface water layer. Significant amounts of subglacial water have not been observed outside the period from July to mid-September and never at GF3 in the outer sill region (Figure 4a). Subglacial water forms when buoyant subglacial freshwater enters the fjord at depths

21699291, 2018, 11, Downloaded from https://agupubs.onlinelibrary.wiley.com/doi/10.1029/2018JC014549 by EVIDENCE AID - BELGIUM, Wiley Online Library on [20/02/2023]. See the Terms and Conditions (https://onlinelibrary.wiley.com/terms-and-conditions) on Wiley Online Library for rules of use; OA articles are governed by the applicable Creative Commons License

Table 1
GF3 Annual Potential Temperature and Salinity Range in the Period of 2006–2015

Year	θ_{min}	θ_{max}	S_{min}	S_{max}
2006	0.11	5.60	27.36	34.33
2007	−0.38	5.90	24.20	34.07
2008	−1.04	7.26	25.92	34.12
2009	−0.49(−1.43)	5.87(5.58)	28.83(8.78)	34.09(33.57)
2010	−0.35(−1.07)	8.26(3.69)	18.48(5.58)	34.29(33.60)
2011	0.09(−1.55)	7.60(5.53)	19.37(4.48)	34.21(33.80)
2012	−0.57(−1.33)	8.48(4.35)	20.50(6.20)	34.37(33.75)
2013	−0.36(−1.10)	5.49(5.49)	26.92(8.08)	33.99(33.58)
2014	−0.15(−1.64)	8.14(7.13)	23.01(4.80)	33.85(33.59)
2015	−0.38(−1.60)	6.59(2.68)	26.62(5.29)	34.20(33.55)
All	−1.04(−1.64)	8.48(7.13)	18.48(4.48)	34.37(33.80)

Note. In parentheses, the inner time series annual potential temperature and salinity range in the 1- to 300-m depth range for the period of 2009–2015.

in connection with tidewater outlet glaciers and mixes with ambient fjord waters as it ascends toward the surface (Jackson et al., 2017). During the ascent and subsequent transport away from the glacier terminus, the subglacial water is further modified by glacial ice melt. In Godthåbsfjord, the glacial melt modification occurs during the transport away from the glaciers (Bendtsen et al., 2015). The fate of subglacial water as it approaches the outer sill region is still not described in detail. However, summer surface layer temperatures observed at GF3 are relatively low compared to those found at the coast, which suggests that subglacial water and summer surface water mixes before entering the outer sill region. This is further supported by the relatively high surface salinities observed in the surface layer at GF3.

During summer and autumn, a warm and relatively saline sill region water is found in the inner part of the fjord where it occupies the intermediate layer of the main fjord branch beneath the cold and relatively fresh subglacial water and above the relatively cold and saline basin water. This water mass has been traced from the inner part of the fjord to its origins in the outer sill region, where it is formed by diapycnal mixing driven by tides. Several water masses contribute to its characteristics, for example, summer surface water, subglacial water, coastal water, summer coastal water (sCW), and subpolar mode water. During winter, sill region water is replaced by basin water, which is lifted into the intermediate layer by a dense coastal inflow.

Table 1 shows annual ranges of potential temperature and salinity at GF3 and the inner fjord for the period of 2006–2015. Water masses are generally colder and fresher in the inner part of the fjord than in the outer part. However, with one exception in 2013, the upper temperature limits were the same at the two sites (5.49 °C).

In the outer part of the fjord, the lowest temperature (−1.04 °C) was observed on 5 April 2008 at a depth of 281 m in a period characterized by local air temperatures around −20 °C. We link this deep temperature minimum to an inflow of cold coastal water. In contrast, the highest temperature (8.47 °C) was observed at the sea surface on 12 July 2012, the same day that the greatest GIS melt event in recent times was observed/reported (Nghiem et al., 2012). The lowest salinity (18.48) was observed at the surface on 25 August 2010. Year 2010 was characterized by record high annual mean air temperatures in the area around Nuuk and on the southwest coast of Greenland (Cappelen, 2018). Finally, the highest bottom water temperature (4.5 °C) was observed on 21 December 2010, just above the bottom at a depth of 350 m. The highest salinity (34.37) was measured at 249-m depth on 15 March 2012.

In the inner part of the fjord, the annual lower and upper temperature limits were generally observed in the surface layer, except on one occasion on 5 November 2010, when the highest temperature (3.69 °C) was observed at a depth of 150 m. The observed temperature and salinity ranges characterized the different water masses and modifications in the fjord and particular periods with strong atmospheric forcing as discussed below.

3.2.1. Monthly Climatology at the Fjord Entrance (GF3)

Figures 5a and 5b show monthly averaged fjord entrance (GF3) property isopleths and their standard deviations from October 2005 to September 2013. Figure 5b reveals that the most saline waters are usually observed at depth in the period from February to April. During the same period, temperatures are observed to decrease (Figure 5a). This suggests that the timing of coastal inflows to Godthåbsfjord determines their temperature properties. Early coastal inflows to the fjord are more likely to be warm, in contrast to late inflows, which tend to be colder.

Figure 5a reveals a close coupling between water temperature found in the 0- to 50-m depth range and the temperature of the local atmosphere. Below 150-m depth, there is a lag between air and water temperatures as the water temperatures become increasingly decoupled from the local atmospheric forcing and more influenced by coastal inflows. Minimum temperatures in the entire water column occur during March–April, except for the near-surface layer (10 m) where the coldest temperatures are observed during January–March. Maximum temperatures are usually reached in July to September at depths shallower than 100 m. Below 100-m depth, maximum temperature occurs in October and is usually associated with coastal inflows associated with an increase in salinity.

21699291, 2018, 11, Downloaded from https://agupubs.onlinelibrary.wiley.com/doi/10.1029/2018JC014549 by EVIDENCE AID - BELGIUM, Wiley Online Library on [20/02/2023]. See the Terms and Conditions (https://onlinelibrary.wiley.com/terms-and-conditions) on Wiley Online Library for rules of use; OA articles are governed by the applicable Creative Commons License

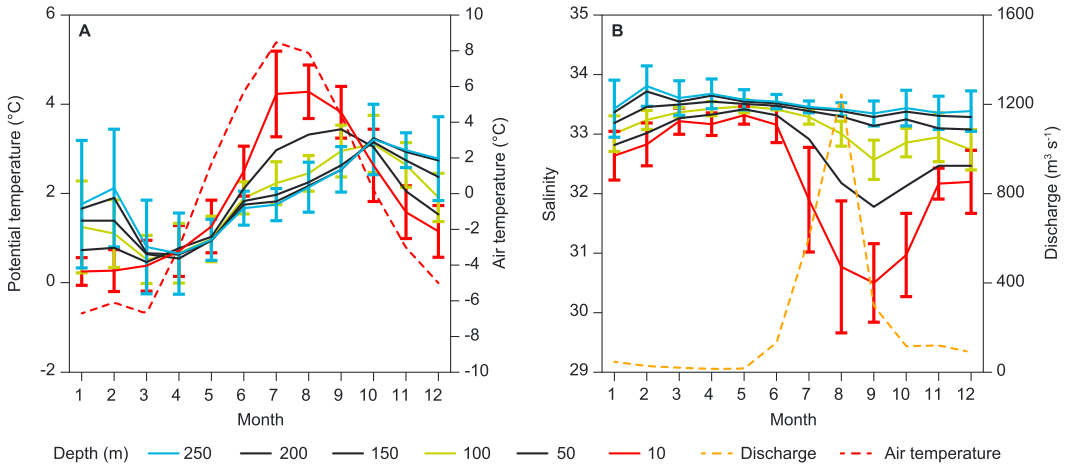

Figure 5. Monthly mean water (a) potential temperature (°C) and (b) salinity isopleths at GF3, for the period of October 2005 to September 2013. Depth: 10 m (red), 50 m (black), 100 m (green), 150 m (black), 200 m (black), and 250 m (blue). Standard deviation is shown for 10-, 100-, and 250-m depth in (a) and (b). (a) Monthly mean temperature for Nuuk in the period October of 2005 to September 2013 (dashed red line). (b) Monthly mean discharge for Lake Tasersuaq in the period of August 2008 to July 2009 (orange dashed line).

We also observe a close coupling between the water column properties in the outer sill region and the freshwater runoff from GIS (Figure 5b). The salinity minimum in the depth range between 10 and 100 m occurs in September, and it closely follows the seasonal freshwater runoff maximum to the fjord with a phase lag of less than a month. In contrast, the salinity minimum below 100-m depth occurs in December/January. Reduced freshwater runoff has an almost instantaneous impact in the upper 100 m, whereas the deeper parts continue to freshen in autumn due to the prevailing circulation system (Mortensen et al., 2011, 2014). This ongoing freshening of the deeper layers continues until the dense coastal inflow season starts in winter.

3.3. Variability in the Outer and Inner Fjord

Depth-time contour plots of potential temperature and salinity were constructed for the two fjord sites (Figures 6 and 7), and time series showed considerable seasonal and interannual variation in both parameters.

At both sites, the warmest intermediate water mass arrived at the end of summer 2010, when the highest temperatures (>4 °C) were observed in the outer part of the fjord (Figure 6). These relatively warm conditions were first terminated by the cold winter at the start of 2012, when subzero temperatures were observed throughout the water column in the outer part of the fjord. The intermediate mean temperature level then underwent a drop, overlaid with regular seasonal oscillations in the outer (inner) part of the fjord, with the coldest periods observed in late winter (spring) and warmest in late autumn (start winter), respectively. The cold winter in the start of 2015 further lowered the mean temperature and caused the coldest period (<1 °C) observed in spring in the inner part of the fjord. A colder period also prevailed between 2008 and 2010 at intermediate depth, where temperatures in the range of 1–2 °C were observed in the inner part. The outer time series was characterized by a cold winter at the start of 2008. Before 2008, seasonal temperatures were within the range of 0–3.5 °C.

Differences in the depth-time potential temperature distributions between the outer and inner parts of the fjord are related to the fjord's circulation system, local atmospheric forcing, freshwater discharge, and ice melt (Figures 6a and 6b). In the outer part of the fjord the close coupling between the upper 100 m of the water column and the atmosphere results in deep-reaching tongues of warm water in summer and cold tongues in winter and the seasonal deepening of the isotherms is caused by tidal diapycnal mixing. Conversely, in the inner part of the fjord, the layer influenced by the atmosphere is shallower and restricted to the upper 5–20 m of the water column as vertical mixing is weaker (Mortensen et al., 2011, 2014). During summer, the upper stratification is maintained by runoff (estuarine circulation), subglacial freshwater discharge (subglacial circulation), and glacial ice melt. During winter the upper stratification is a result of sea ice cover and (dense) coastal inflow (Meire et al., 2016; Mortensen et al., 2014). Two circulation modes are associated with lifting of

21699291, 2018, 11, Downloaded from https://agupubs.onlinelibrary.wiley.com/doi/10.1029/2018JC014549 by EVIDENCE AID - BELGIUM, Wiley Online Library on [20/02/2023]. See the Terms and Conditions (https://onlinelibrary.wiley.com/terms-and-conditions) on Wiley Online Library for rules of use; OA articles are governed by the applicable Creative Commons License

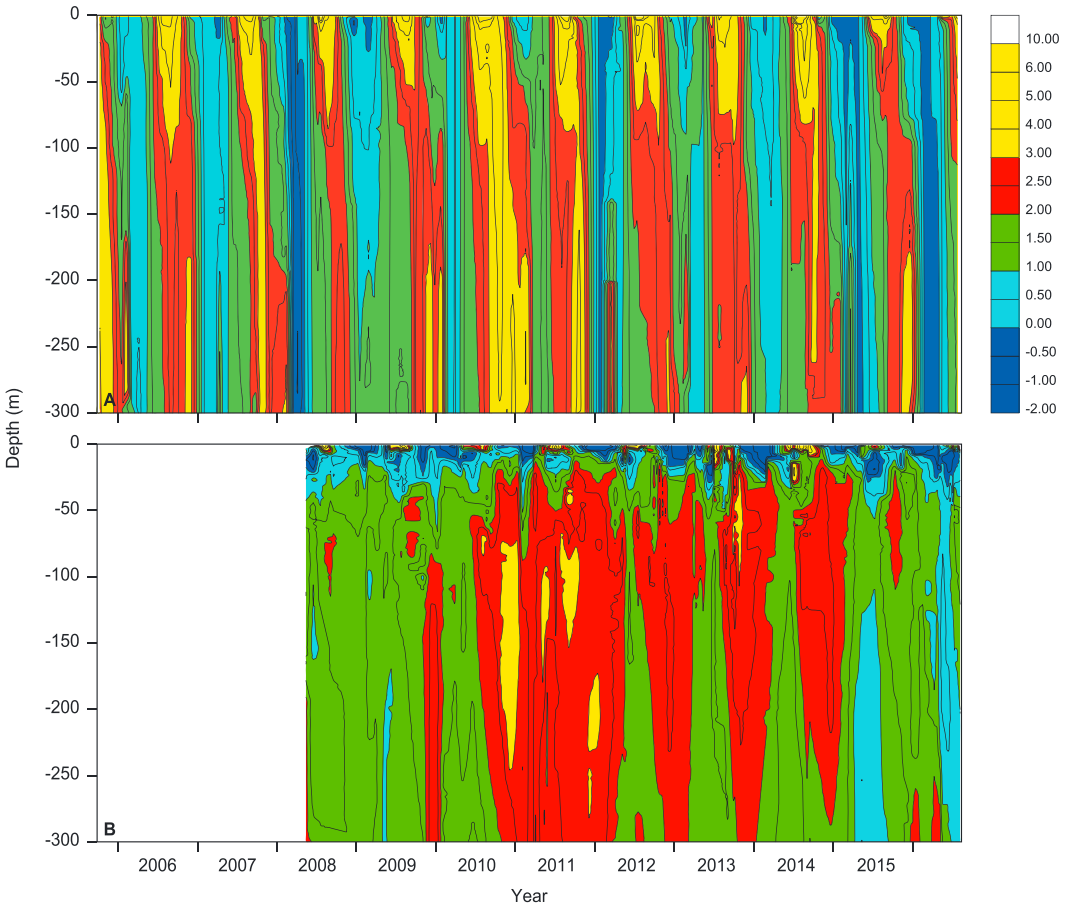

Figure 6. Depth-time contour plots of potential temperature for (a) outer time series (GF3) and (b) inner time series during the period of October 2005 to July 2016.

isotherms near the sea surface in the inner part of the fjord: dense coastal inflows during winter and subglacial circulation during summer, and both contribute to maintaining the 1 °C isotherm at ~20-m depth for at least 8 years, that is, from 2008 to winter 2016. Also, in the intermediate water masses, a distinct difference between the inner and outer part can be observed with a much narrower seasonal temperature range in the inner part and where subzero temperatures are frequently observed in the outer part of the fjord but never to reach the inner part.

The depth-time contour plot of salinity for the two sites shows the buildup of a fresh surface layer during summer and a general deepening of isohalines starting in late spring, followed by episodic saline inflows in autumn and winter, resulting in a lifting of isohalines toward the surface (Figure 7). Many of the episodic coastal inflows observed in the outer part of the fjord are apparently not strong enough to influence the inner part significantly. During winter, the surface layer in the outer fjord is characterized by salinities above 33.0 and a weak stratification, whereas the inner part of the fjord is characterized by salinities below 32.5. The highest salinity at intermediate depth measured at the 150-m isobath was observed on 25 January 2010 and 10 May 2011 in the outer and inner parts, respectively. The reduced variability in the salinity distribution inner part is manifested as smoother salinity-contours (Figure 7b).

The time series of potential temperature and salinity for the outer and inner fjord were analyzed in detail at three discrete depths (Figure 8). These depths represent the surface layer (2 m), the layer influenced by glacial melt and subglacial freshwater discharge (20 m), and the layer containing relatively warm water masses connected to the glacial melt domain (150 m).

The surface layer is characterized by a seasonal signal. During winter, properties are more or less the same in the inner and outer parts of the fjord: a temperature of ~ −1–0 °C and a salinity of 32–33 with slightly lower

21699291, 2018, 11, Downloaded from https://agupubs.onlinelibrary.wiley.com/doi/10.1029/2018JC014549 by EVIDENCE AID - BELGIUM, Wiley Online Library on [20/02/2023]. See the Terms and Conditions (https://onlinelibrary.wiley.com/terms-and-conditions) on Wiley Online Library for rules of use; OA articles are governed by the applicable Creative Commons License

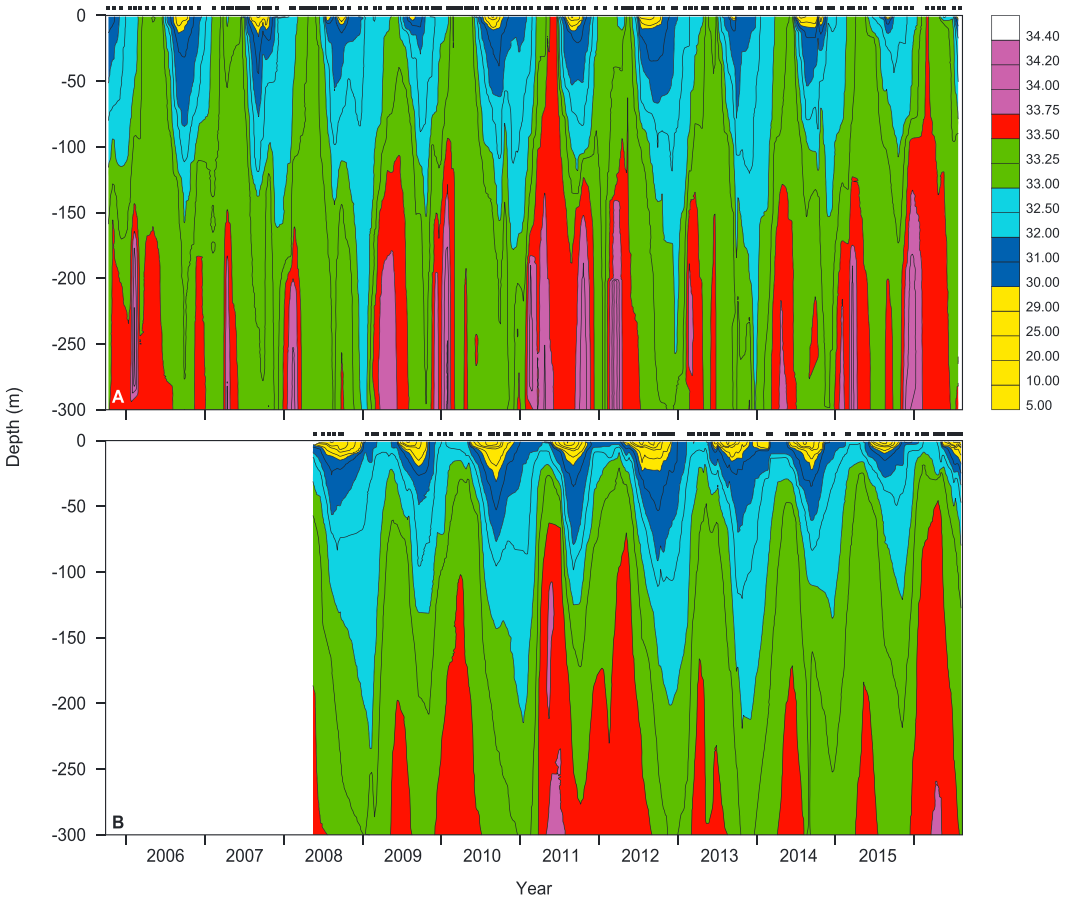

Figure 7. Depth-time contour plots of salinity for (a) the outer time series (GF3) and (b) inner time series during the period of October 2005 to July 2016 (station occupations are indicated with dots).

temperature in the inner part and slightly higher salinity in the outer part. During summer, differences between the two regions are more pronounced because runoff, subglacial freshwater discharge, and glacial ice melt strongly influence surface conditions. Temperatures vary between 2 and 6 °C in the inner part, while in the outer part, the surface layer is warmer with temperatures ranging from 2 to 9 °C. The salinity also shows pronounced differences with salinities ranging from 5 to 15 in the inner part while a range of 20 to 31 in the outer part. For example, the years 2010 and 2012 were characterized by elevated freshwater discharge (Motyka et al., 2017).

The layer containing the 20-m isobath is characterized by a seasonal signal with the exception of the inner temperature time series, which shows high-frequency variation overlaying the seasonal signal. During winter, salinity is more or less the same ~33 in the inner and outer parts of the fjord with slightly higher salinities in the outer part. Temperatures vary between 0 and 1 °C in the outer part, whereas temperatures vary between 1 and 2 °C in the inner parts. During summer, the salinity ranges are 30–32 and 29–32 for the outer and inner parts, respectively. The temperature is around 4 °C in the outer part and 0 °C in the inner part of the fjord.

The layer containing the 150-m isobath is part of the fjord's glacial melt domain (Figures 8e and 8f) and is characterized by similar seasonal signals in the outer and inner part of the fjord. The salinity time series show a seasonal range between 32.5 and 34 with minimum values during autumn. The majority of the saline dense coastal inflows (seen as salinity maxima's during winter in the outer time series) are slightly fresher when they arrive in the inner part of the fjord. The seasonal temperature range in the outer part of the fjord is found to vary between −1 and 4.5 °C, whereas it varies between 1 and 4 °C in the inner part of the fjord. The major difference between the outer and inner part of the fjord is that the cold winter temperatures experienced in the outer part never arrive at the inner part of the fjord.

21699291, 2018, 11, Downloaded from https://agupubs.onlinelibrary.wiley.com/doi/10.1029/2018JC014549 by EVIDENCE AID - BELGIUM, Wiley Online Library on [20/02/2023]. See the Terms and Conditions (https://onlinelibrary.wiley.com/terms-and-conditions) on Wiley Online Library for rules of use; OA articles are governed by the applicable Creative Commons License

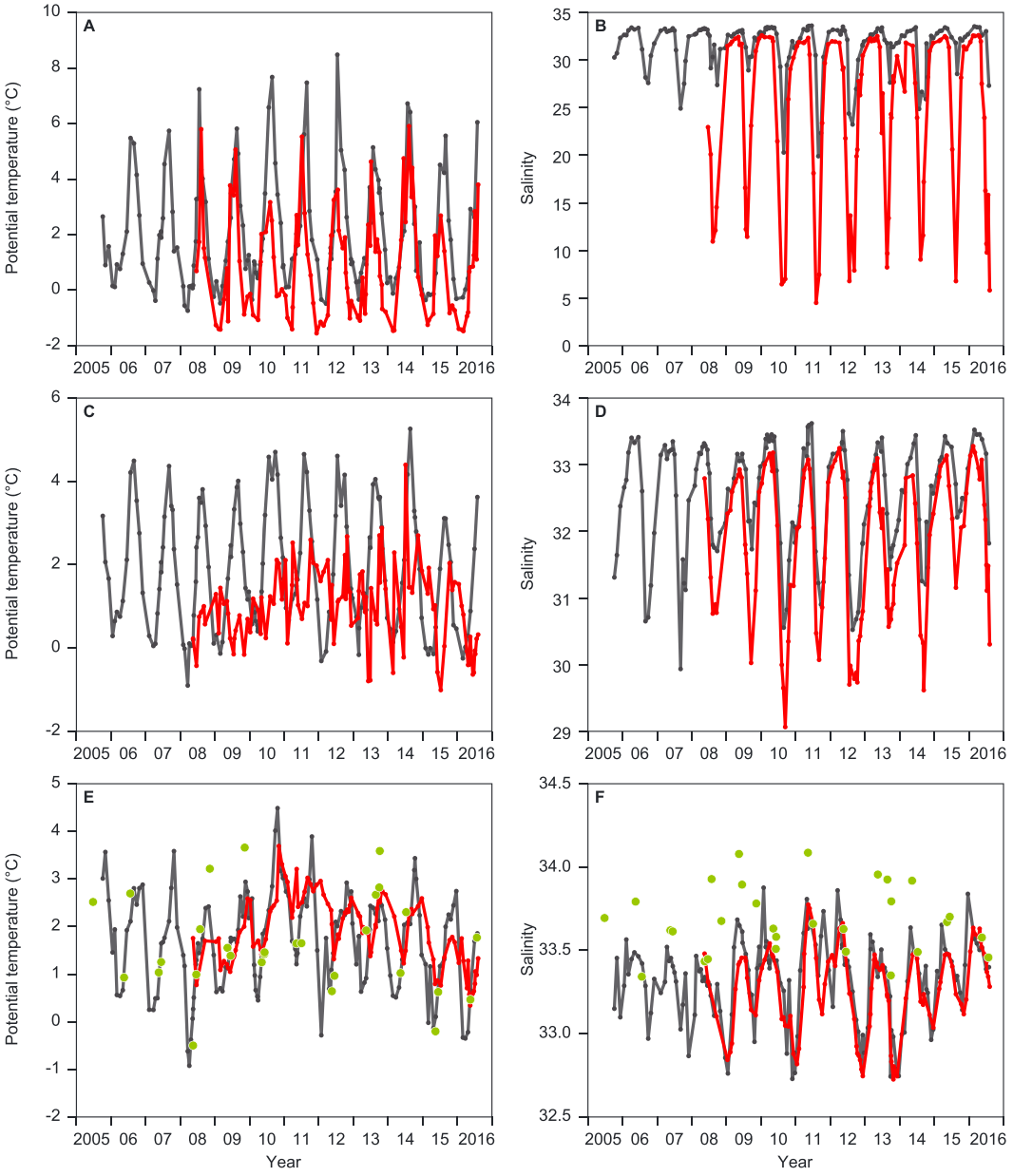

Figure 8. Time series of potential temperature and salinity for the outer time series (GF3, black line) and the inner time series (red line) for three depth levels: (a and b) 2 m, (c and d) 20 m, and (e and f) 150 m, respectively, in the period of October 2005 to July 2016. Time series for the coastal station (FB1), 150-m depth, is shown as green points in (e) and (f). (Notice the different temperature and salinity scales used by the different depth levels.)

3.4. The Coast-Fjord-Glacier Connection

In this section, we focus on the 150-m depth isobaths, which provides important information on the connection of relative warm water between the open ocean and GIS (Figures 8e and 8f). Coastal temperatures observed during the period from May to June/July at FB1 were similar to those observed in the outer part of the fjord (GF3), whereas coastal temperatures in autumn were, generally, 1 °C warmer. In contrast, salinities were observed to be higher at the coast than in the outer part of the fjord year-round.

In the fjord, our observations reveal that low subsurface winter temperatures in the outer part rarely reach the inner part of the fjord (Figure 8e). However, high temperatures in summer and autumn are communicated more easily through the subsurface circulation system. This is also observed in the salinity time series,

21699291, 2018, 11, Downloaded from https://agupubs.onlinelibrary.wiley.com/doi/10.1029/2018JC014549 by EVIDENCE AID - BELGIUM, Wiley Online Library on [20/02/2023]. See the Terms and Conditions (https://onlinelibrary.wiley.com/terms-and-conditions) on Wiley Online Library for rules of use; OA articles are governed by the applicable Creative Commons License

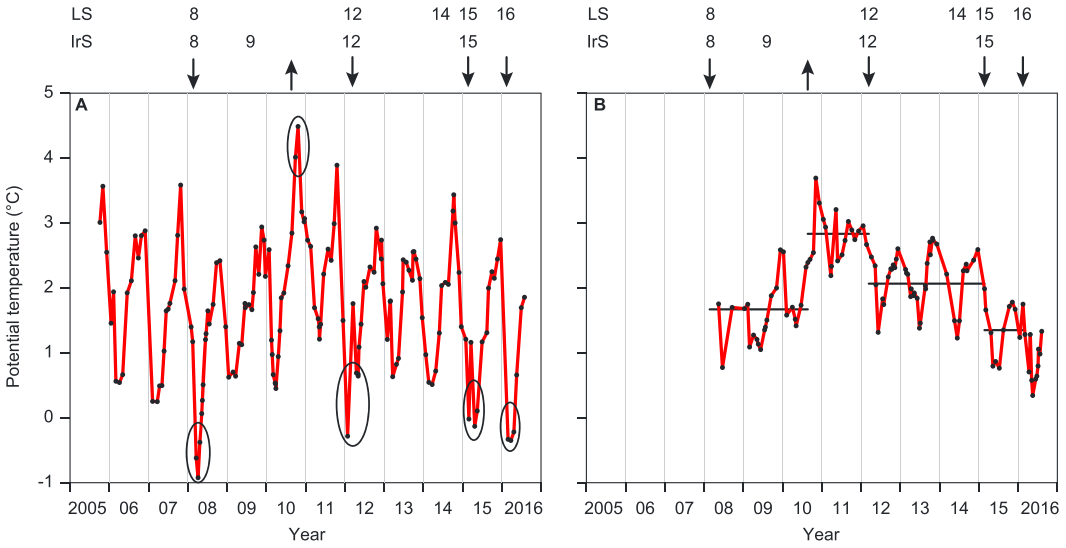

Figure 9. Time series of potential temperature for (a) the outer time series (GF3) and (b) the inner time series at 150-m depth, for the period of October 2005 to July 2016. The arrows and closed ellipses indicate temperatures events observed at station GF3 (arrow direction: down = cold event; up = warm event). The horizontal line segments indicate the mean temperature between two consecutive, temperature events. Years of observed deep convection in the Labrador Sea (LS) and Irminger Sea (IrS) are indicated above the panels. See text for explanation.

where the saline water in the outer part never reaches the inner part during winter. We suggest that these differences can be explained by the seasonal circulation system where the subsurface seasonal temperature range in the inner part of the fjord is damped and reduced by a factor of ~2, relative to the range found at the entrance of the fjord. During winter, the temperature in the intermediate layer is therefore warmer in the inner part of the main fjord branch than in the outer part.

In our effort to explain the temperature variation observed in the intermediate layer in the inner part of the fjord, which is a potential source for glacial melt, we hypothesize that mean temperature shifts in the inner part of the fjord are initiated by either cold or warm temperature events in the outer part of the fjord. In Figure 9, we show time series of potential temperature for the outer fjord (GF3) and the inner fjord at 150-m depth for the period from October 2005 to July 2016. Arrows indicate five events: 2008, 2010, 2012, 2015, and 2016. Four of these are associated with cold winter events (2008, 2012, 2015, and 2016), while 2010 is associated with a warm summer event. The associated response in the inner part to temperature events in the outer part is visualized in Figure 9b by horizontal line segments around which the seasonal signal oscillates. The horizontal line segments are determined by the calculated mean temperature between two consecutive events. Thus, the arrival of a new temperature event in the outer part of the fjord might forecasts a shift in mean temperature in the inner part. The direction of the shift depends on the temperature of the event.

The TS-properties reveals that the water mass associated with the cold temperature events in the outer part of the fjord (Figure 9a) is coastal water and it is so voluminous that it occupies the entire water column at GF3. In effect, it blocks the entrance to the fjord for potential dense coastal inflows in this period. This gives rise to later coastal inflows, which generally are colder and change the future mean temperature in the fjord. The water mass associated with the warm temperature event is summer coastal water, which enters the fjord in autumn. We traced the arrival of the elevated temperature in autumn 2010 back to a water mass found in the upper water column on the coast, that is, summer coastal water, as identified by its temperature and salinity and the progress of isohalines below ~80 m (Figure 7). Both water masses associated with temperature events are considered as local water masses formed on the southwest Greenland continental shelf.

We note that the cold winter events in 2008, 2012, 2015, and 2016 in the outer part of the fjord are observed during years when deep convection is observed in the Irminger Sea (de Jong & de Steur, 2016) and Labrador Sea (Yashayaev & Loder, 2016, 2017), as indicated in Figure 9a. As a response to the cold winter events, the mean temperature in the inner part of the fjord experiences a shift toward lower temperatures (Figure 9b).

21699291, 2018, 11, Downloaded from https://agupubs.onlinelibrary.wiley.com/doi/10.1029/2018JC014549 by EVIDENCE AID - BELGIUM, Wiley Online Library on [20/02/2023]. See the Terms and Conditions (https://onlinelibrary.wiley.com/terms-and-conditions) on Wiley Online Library for rules of use; OA articles are governed by the applicable Creative Commons License

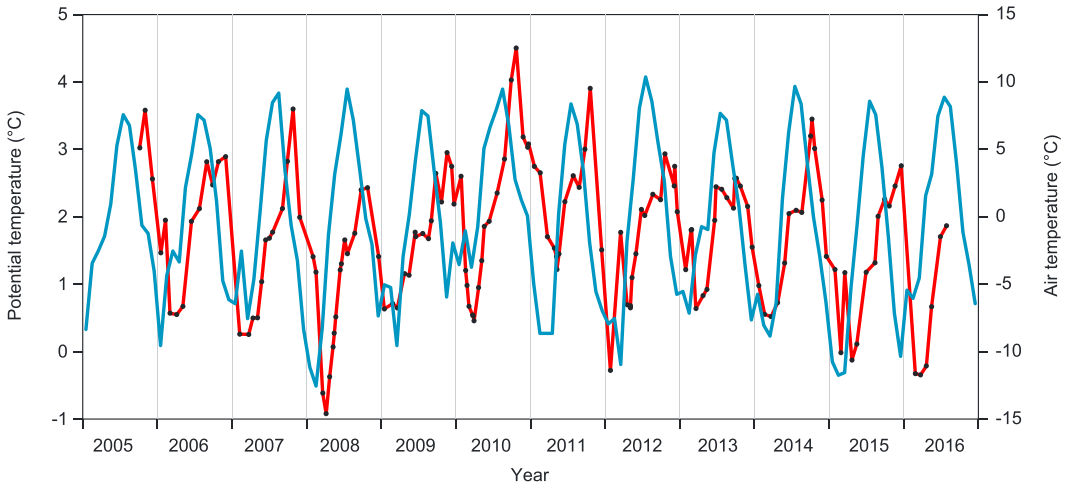

Figure 10. Time series of potential temperature at 150-m depth at the outer time series (GF3, red line) and monthly mean air temperature (Nuuk, blue line) for the period of 2005–2016.

In contrast, the warm summer event in 2010 prompted a significant mean temperature rise in this part of Godthåbsfjord (Figure 9b). A record high annual air temperature in 2010 characterized the area around Nuuk and on the southwest coast of Greenland (Cappelen, 2011). Other studies by de Jong and de Steur (2016) and Yashayaev and Loder (2016, 2017) also observed elevated temperatures in the Labrador Sea and the Irminger Sea in 2010 and 2011, and open water convection only reached shallow depths. Motyka et al. (2017) showed that the 2010–2014 Narsap Sermia retreat could be linked primarily to this temperature increase in the intermediate layer, resulting in increased submarine melt. Our time series suggest that the high mean temperature level between 2010 and 2012 may explain this 2010–2014 Narsap Sermia retreat. This high mean temperature level can be associated with the warm summer event in 2010 at intermediate depth in the outer part of the fjord.

We link the occurrence of the aforementioned cold and warm temperature events in the intermediate layer in the outer fjord to coastal water masses and local atmospheric forcing. Figure 10 shows time series of potential temperatures at 150-m depth for the outer part of the fjord and monthly mean air temperatures for Nuuk (Cappelen, 2018). Cold atmospheric conditions are occurring during periods with cold events, whereas the warm event in 2010 was caused by a combination of a weak winter and a relatively long, warm summer. The present data set shows that coastal water masses and local atmospheric forcing is closely related and may likely be responsible for the interannual mean temperature shift observed near the tidewater outlet glaciers in Godthåbsfjord.

The TS-properties of the warm and saline water mass associated with the second highest temperature peak in 2011 in the outer fjord was identified as modified subpolar mode water (Figure 9a). Upon arrival in the inner fjord, it affects the seasonal signal (Figure 9b) but does not gives rise to a mean temperature shift. Our time series presented here show that mean temperature changes in the inner fjord are associated with local coastal water masses, whereas the regional water mass (subpolar mode water) affects the seasonal signal.

In the associated salinity time series, Figure 11a, we observe that saline water is linked to the cold winter events, whereas the warm summer event in 2010 is associated with low-saline water. The characteristic periods observed in the temperature time series above are not observed in the salinity time series. However, the salinity time series can be divided into three distinct periods: 2005–2008, 2009–2012, and 2013–2016. The first period (2005–2008) was characterized by a seasonal signal, overlaying a linear freshening trend. The second period (2009–2012) was characterized by elevated winter salinities with large seasonal fluctuations. During the third period (2013–2016), the seasonal signal returned, this time overlaying a linear trend with increasing salinities. At the inner time series, a similar pattern was observed but with a reduced variability (Figure 11b).

The way freshwater enters the fjord system has implications for the downstream fjord circulation. The period 2010–2012 was characterized by enhanced freshwater discharge to the fjord (Langen et al., 2015; Motyka

21699291, 2018, 11, Downloaded from https://agupubs.onlinelibrary.wiley.com/doi/10.1029/2018JC014549 by EVIDENCE AID - BELGIUM, Wiley Online Library on [20/02/2023]. See the Terms and Conditions (https://onlinelibrary.wiley.com/terms-and-conditions) on Wiley Online Library for rules of use; OA articles are governed by the applicable Creative Commons License

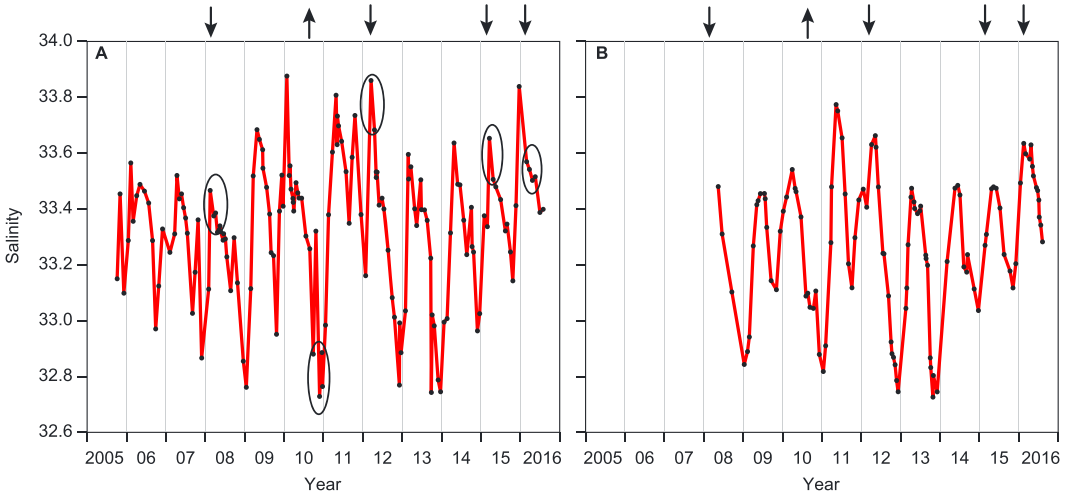

Figure 11. Time series of salinity for (a) the outer time series (GF3) and (b) the inner time series at 150-m depth respectively, for the period of October 2005 to July 2016. The arrows and closed ellipses indicate temperature events observed at station GF3 (arrow direction: down = cold event; up = warm event).

et al., 2017). In the outer part of the fjord, we observed intensified summer surface stratification during the same period (Figures 8b and 8d). In a Northeast Greenland fjord, an increased runoff was found to result in a similar intensified summer stratification and a reduction of the surface layer thickness (Bendtsen et al., 2014). A stronger stratification at GF3 tends to reduce the vertical diapycnal mixing of low-saline surface water in the outer sill region. This would lead to an enhanced freshwater transport out of the fjord, and less recirculated freshwater will mix into the sill region water. This could form a stabilizing feedback that can limit the freshening of the fjord. A similar feedback may operate in other fjords along the coast as well.

4. Summary and Conclusions

This study presents long-term seasonal hydrographic observations from Godthåbsfjord, which is one of Greenland's largest tidewater outlet glacier fjords. The time series at the outer part of the fjord (GF3) revealed that the seasonal timing of dense coastal inflows has a major influence on the water mass characteristics during spring and summer. Early coastal inflows are generally warmer than inflows later in the winter. Processes inside the fjord further play a crucial role in damping heat fluxes to the tidewater outlet glaciers.

The two fjord time series revealed significant amounts of subglacial water mainly in the period from July to mid-September and no subglacial water at GF3 near the fjord entrance. The relatively low surface layer temperatures observed at GF3 compared to those found at the coast suggest that subglacial water is mixed with fresh surface water before it reaches the outer sill region. In the outer sill region all the fjord's different freshwater sources are further mixed, which results in a surface water mass with a relatively weak freshwater imprint. If this phenomenon is a general feature of fjords around Greenland, it will have implications for the role of freshening from GIS on the North Atlantic's deepwater formation regions, because freshwater will mix with local water masses before reaching these sites.

We observed that the inner fjord acts as a large heat reservoir during winter, when cold water masses observed in the outer part of the fjord never reach the inner part of the fjord. Heat storage in the fjord is linked to the seasonal circulation system of the fjord.

Our observations show interannual changes in the mean temperatures of water masses in the glacial melt domain, that is, water masses responsible for the melt of the tidewater outlet glaciers. Changes in the mean temperature are related to temperature events changing the characteristics of intermediate water masses in the outer part of the fjord. Cold winter events have been observed to lower and warm summer events to increase the mean temperature for several years in the inner parts of the fjord, respectively. We show that these temperature events are predominantly caused by local coastal water masses and can be related to local atmospheric forcing.

21699291, 2018, 11, Downloaded from https://agupubs.onlinelibrary.wiley.com/doi/10.1029/2018JC014549 by EVIDENCE AID - BELGIUM, Wiley Online Library on [20/02/2023]. See the Terms and Conditions (https://onlinelibrary.wiley.com/terms-and-conditions) on Wiley Online Library for rules of use; OA articles are governed by the applicable Creative Commons License

Furthermore, our observations uncover a stabilizing feedback mechanism that may limit the freshening of the fjord and this feedback may operate in similar fjords along the coast. Increased runoff and, thereby, stronger stratification tends to reduce vertical diapycnal mixing of low-saline surface water in the outer sill region. This in turn may lead to enhanced freshwater transport out of the fjord and less recirculated freshwater into the fjord.

Thus, further understanding on how cold/warm events and increased freshwater discharge influences the spreading of freshwater to the coastal and open ocean system is critical.

Acknowledgments

This study received financial support from the Greenland Climate Research Centre and Greenland Research Council. Funding was also provided by the DEFROST project of the Nordic Centre of Excellence program "Interaction between Climate Change and the Cryosphere." This study was conducted in collaboration with the MarineBasis Nuuk monitoring program, part of Greenland Ecosystem Monitoring (GEM), and forms a contribution to the Arctic Science Partnership (ASP). We would like to thank Flemming Heinrich, Lars Heilmann, Louise Mølgaard, Thomas Krogh, Else Ostermann, and many others for field assistance and Hr. Lund for linguistic help. Monthly GF3 data and May 2013 length section data from the Greenland Ecosystem Monitoring Programme (www.g-e-m.dk) were provided by the Greenland Institute of Natural Resources, Nuuk, Greenland, in collaboration with Department of Bioscience, Aarhus University, Denmark. Data used from the inner part of Godthåbsfjord are available from the International Council for the Exploration of the Sea (ICES, www.ices.dk).

References

Arendt, K. E., Juul-Pedersen, T., Mortensen, J., Blicher, M. E., & Rysgaard, S. (2013). A 5-year study of seasonal patterns in mesozooplankton community structure in a sub-Arctic fjord reveals dominance of *Microsetella norvegica* (Crustacea, Copepoda). *Journal of Plankton Research*, *35*(1), 105–120. https://doi.org/10.1093/plankt/fbs087

Bendtsen, J., Mortensen, J., Lennert, K., & Rysgaard, S. (2015). Heat sources for glacial ice melt in a west Greenland tidewater outlet glacier fjord: The role of subglacial freshwater discharge. *Geophysical Research Letters*, *42*, 4089–4095. https://doi.org/10.1002/2015GL063846

Bendtsen, J., Mortensen, J., & Rysgaard, S. (2014). Seasonal surface layer dynamics and sensitivity to runoff in a high Arctic fjord (Young Sound/Tyrolerfjord, 74°N). *Journal of Geophysical Research: Oceans*, *119*, 6461–6478. https://doi.org/10.1002/2014JC010077

Boone, W., Rysgaard, S., Carlson, D. F., Meire, L., Kirillov, S., Mortensen, J., et al. (2018). Coastal freshening prevents fjord bottom water renewal in Northeast Greenland: A mooring study from 2003 to 2015. *Geophysical Research Letters*, *45*, 2726–2733. https://doi.org/10.1002/2017GL076591

Cappelen, J. (2011). DMI annual climate data collection 1873–2010, Denmark, The Faroe Islands and Greenland - with graphics and Danish summary, Danish Meteorological Institute Tech. Rep. No. 11-04, 23pp.

Cappelen, J. (2018). Greenland-DMI historical climate data collection 1784–2017, Danish Meteorological Institute Rep. No. 18-04.

Carroll, D., Sutherland, D. A., Shroyer, E. L., Nash, J. D., Catania, G. A., & Stearns, L. A. (2017). Subglacial discharge-driven renewal of tidewater glacier fjords. *Journal of Geophysical Research: Oceans*, *122*, 6611–6629. https://doi.org/10.1002/2017JC012962

de Jong, M. F., & de Steur, L. (2016). Strong winter cooling over the Irminger Sea in winter 2014–2015, exceptional deep convection, and the emergence of anomalously low SST. *Geophysical Research Letters*, *43*, 7106–7113. https://doi.org/10.1002/2016GL069596

Gladish, C., Holland, D., & Lee, C. (2015). Oceanic boundary conditions for Jakobshavn Glacier: Part II. Provenance and sources of variability of Disko Bay and Ilulissat Icefjord waters, 1990–2011. *Journal of Physical Oceanography*, *45*(1), 33–63. https://doi.org/10.1175/JPO-D-14-0045.1

Holland, D. M., Thomas, R. H., DeYoung, B., Ribergaard, M. H., & Lyberth, B. (2008). Acceleration of Jakobshavn Isbræ triggered by warm subsurface ocean waters. *Nature Geoscience*, *1*(10), 659–664. https://doi.org/10.1938/ngeo316.

Jackson, R. H., Shroyer, E. L., Nash, J. D., Sutherland, D. A., Carroll, D., Fried, M. J., et al. (2017). Near-glacier surveying of a subglacial discharge plume: Implications for plume parameterizations. *Geophysical Research Letters*, *44*, 6886–6894. https://doi.org/10.1002/2017GL073602

Jackson, R. H., Straneo, F., & Sutherland, D. A. (2014). Externally forced fluctuations in ocean temperature at Greenland glaciers in non-summer months. *Nature Geoscience*, *7*(7), 503–508.

Juul-Pedersen, T., Arendt, K. E., Mortensen, J., Blicher, M. E., Søgaard, D. H., & Rysgaard, S. (2015). Seasonal and interannual phytoplankton production in a sub-Arctic tidewater outlet glacier fjord, SW Greenland. *Marine Ecology Progress Series*, *524*, 27–38. https://doi.org/10.3354/meps11174

Krawczyk, D. W., Witkowski, A., Juul-Pedersen, T., Arendt, K. E., Mortensen, J., & Rysgaard, S. (2015). Microplankton succession in a SW Greenland tidewater glacial fjord influenced by coastal inflows and runoff from the Greenland Ice Sheet. *Polar Biology*, *38*, 1515–1533. https://doi.org/10.1007/s00300-015-1715-y

Langen P. L., Mottram, R. H., Christensen, J. H., Boberg, F., Rodehacke, C. B., Stendel, M., et al. (2015). Quantifying energy and mass fluxes controlling Godthåbsfjord freshwater input in a 5 km simulation (1991–2012). *Journal of Climate*, *28*, 3694–3713. https://doi.org/10.1175/JCLI-D-14-00271.1

Meire, L., Mortensen, J., Meire, P., Juul-Pedersen, T., Sejr, M. K., Rysgaard, S., et al. (2017). Marine-terminating glaciers sustain high productivity in Greenland fjords. *Global Change Biology*, *23*, 5344–5357. https://doi.org/10.1111/gcb.13801

Meire, L., Mortensen, J., Rysgaard, S., Bendtsen, J., Boone, W., Meire, P., et al. (2016). Spring bloom dynamics in a subarctic fjord influenced by tidewater outlet glaciers (Godthåbsfjord, SW Greenland). *Journal of Geophysical Research: Biogeosciences*, *121*, 1581–1592. https://doi.org/10.1002/2015JG003240

Mortensen, J., Bendtsen, J., Lennert, K., & Rysgaard, S. (2014). Seasonal variability of the circulation system in a west Greenland tidewater outlet glacier fjord, Godthåbsfjord (64°N). *Journal of Geophysical Research: Earth Surface*, *119*, 2591–2603. https://doi.org/10.1002/2014JF003267

Mortensen, J., Bendtsen, J., Motyka, R. J., Lennert, K., Truffer, M., Fahnestock, M., et al. (2013). On the seasonal freshwater stratification in the proximity of fast-flowing tidewater outlet glaciers in a sub-Arctic sill fjord. *Journal of Geophysical Research: Oceans*, *118*, 1382–1395. https://doi.org/10.1002/jgrc.20134

Mortensen, J., Lennert, K., Bendtsen, J., & Rysgaard, S. (2011). Heat sources for glacial melt in a subarctic fjord (Godthåbsfjord) in contact with the Greenland Ice Sheet. *Journal of Geophysical Research*, *116*, C01013. https://doi.org/10.1029/2010JC006528

Motyka R. J., Cassotto, R., Truffer, M., Kjeldsen, K. K., van As, D., Korsgaard, N. J., et al. (2017). Asynchronous behavior of outlet glaciers feeding Godthåbsfjord (Nuup Kangerlua) and the triggering of Narsap Sermia's retreat in SW Greenland. *Journal of Glaciology*, *63*(238), 288–308. https://doi.org/10.1017/jog.2016.138

Motyka, R. J., Truffer, M., Fahnestock, M., Mortensen, J., Rysgaard, S., & Howat, I. (2011). Submarine melting of the 1985 Jakobshavn Isbræ floating tongue and the triggering of the current retreat. *Journal of Geophysical Research*, *116*, F01007. https://doi.org/10.1029/2009JF001632

Nghiem, S. V., Hall, D. K., Mote, T. L., Tedesco, M., Albert, M. R., Keegan, K., et al. (2012). The extreme melt across the Greenland ice sheet in 2012. *Geophysical Research Letters*, *39*, L20502. https://doi.org/10.1029/2012GL053611

Richter, A., Rysgaard, S., Dietrich, R., Mortensen, J., & Petersen, D. (2011). Coastal tides in West Greenland derived from tide gauge records. *Ocean Dynamics*, *61*(1), 39–49. https://doi.org/10.1007/s10236-010-0341-z

Rysgaard, S., & Glud, R. N. (2007). Carbon cycling in Arctic marine ecosystems: Case study Young Sound. *Meddelelser om Grønland, Bioscience*, *58*, 160–173.

21699291, 2018, 11, Downloaded from https://agupubs.onlinelibrary.wiley.com/doi/10.1029/2018JC014549 by EVIDENCE AID - BELGIUM, Wiley Online Library on [20/02/2023]. See the Terms and Conditions (https://onlinelibrary.wiley.com/terms-and-conditions) on Wiley Online Library for rules of use; OA articles are governed by the applicable Creative Commons License

Rysgaard, S., Mortensen, J., Juul-Pedersen, T., Sørensen, L. L., Lennert, K., Søgaard, D. H., et al. (2012). High air-sea CO2 uptake rates in nearshore and shelf areas of Southern Greenland: Temporal and spatial variability. *Marine Chemistry*, *128*, 26–33. https://doi.org/10.1016/j.marchem.2011.11.002

Straneo, F., Hamilton, G. S., Sutherland, D. A., Stearns, L., Davidson, F., Hammill, M. O., et al. (2010). Rapid circulation of warm subtropical waters in a major glacial fjord in East Greenland. *Nature Geoscience*, *3*(3), 182–186. https://doi.org/10.1038/NGEO764

Sutherland, D. A., & Straneo, F. (2012). Estimating ocean heat transport and submarine melt rate in Sermilik Fjord, Greenland, using lowered ADCP profiles. *Annals of Glaciology*, *53*(60), 50–58. https://doi.org/10.3189/2012AoG60A050

Tang, K. W., Nielsen, T. G., Munk, P., Mortensen, J., Moller, E. F., Arendt, K. E., et al. (2011). Metazooplankton community structure, feeding rate estimates, and hydrography in a meltwater-influenced Greenlandic fjord. *Marine Ecology Progress Series*, *434*, 77–90. https://doi.org/10.3354/meps09188

Versteegh, E. A. A., Blicher, M. E., Mortensen, J., Rysgaard, S., Als, T. D., & Wanamaker, A. D. Jr. (2012). Oxygen isotope ratios in the shell of *Mytilus edulis*: archives of glacier meltwater in Greenland? *Biogeosciences*, *9*(12), 5231–5241. https://doi.org/10.5194/bg-9-5231-2012

Yashayaev, I., & Loder, J. W. (2016). Recurrent replenishment of Labrador Sea Water and associated decadalscale variability. *Journal of Geophysical Research: Oceans*, *121*, 8095–8114. https://doi.org/10.1002/2016JC012046

Yashayaev, I., & Loder, J. W. (2017). Further intensification of deep convection in the Labrador Sea in 2016. *Geophysical Research Letters*, *44*, 1429–1438. https://doi.org/10.1002/2016GL071668

21699291, 2018, 11, Downloaded from https://agupubs.onlinelibrary.wiley.com/doi/10.1029/2018JC014549 by EVIDENCE AID - BELGIUM, Wiley Online Library on [20/02/2023]. See the Terms and Conditions (https://onlinelibrary.wiley.com/terms-and-conditions) on Wiley Online Library for rules of use; OA articles are governed by the applicable Creative Commons License